THE ASTROPHYSICAL JOURNAL, 255:585–595, 1982 April 15

THE COLORS OF THE PULSATIONS AND FLICKERING OF SY CANCRI DURING OUTBURST

JOHN MIDDLEDITCH[1,2] AND FRANCE A. CÓRDOVA[1,2]
Received 1981 August 24; accepted 1981 November 2

ABSTRACT

The spectra of the short period (~30 s) oscillations and flickering of the dwarf nova SY Cnc have been determined by simultaneously measuring the optical flux in three broad, contiguous spectral bands during an optical outburst of the star. The spectrum of the oscillations rises too rapidly toward short wavelengths to be consistent with any simple thermal model. The colors of the flickering are even more extreme (i.e., more ultraviolet) than those of the pulsations. No timing differences were detected to a fraction of a second between the ultraviolet (U), cyan ($B+V$, or C) and red (R, to 9000 Å) bands of the pulsations; thus, the optical oscillations appear to arise from a single physical location in the binary system. Without a detailed study of a more complicated class of models, which may include recombination radiation from H I, He I, and He II in addition to a thermal model, it is impossible to assign a temperature to the oscillations and thereby determine whether they are produced directly on the white dwarf or in the accretion disk.

Subject headings: stars: dwarf novae — stars: individual — stars: pulsation

I. INTRODUCTION

The nature of the short period (~10–30 s) oscillations found in dwarf novae during their outbursts is unknown at present. It is generally accepted that this time variability is associated with the compact white dwarf member of such binary systems, rather than with the larger red companion star, because of the short time scale of the oscillations and the detection of X-ray pulsations with the same period (Warner 1976; Córdova *et al.* 1980, 1981). The recurrent outbursts are thought to be due to an increase of accretion onto the degenerate dwarf caused either by a sudden onset of flow of material from the late-type companion or by a storage and release mechanism in the disk that the accreting gas forms around the compact star (see the reviews on dwarf novae by Warner 1976; Robinson 1976; and Córdova and Mason 1982).

The short period oscillations do not originate directly from the rotation of the white dwarf by a pulsar-like mechanism, since the frequency has been shown to change by several percent from night to night (see, e.g., Hildebrand *et al.* 1980; also Patterson 1981). In a simultaneous two-color study of the Z Cam type dwarf nova AH Her, Hildebrand, Spillar, and Stiening (1981; hereafter HSS) showed that the ratio of the pulsed ultraviolet amplitude to the pulsed red-infrared amplitude of the rapid oscillations was similar to the same ratio of the unpulsed fluxes from the hot white dwarf HZ 44 and concluded that the temperature of the oscillations was therefore similar to that of HZ 44 (assuming that the spectrum of the pulsations would be consistent with a blackbody). Since the temperature of HZ 44 (~50,000 K, Oke 1974) is higher than the typical accretion disk temperature (~10,000–20,000 K), HSS argued that the short period oscillations originated from the surface of the (accreting) white dwarf, rather than from the accretion disk.

In this paper we use simultaneous three-color data on another Z Cam type variable, SY Cnc, to show that the oscillation amplitude in the intermediate wavelength band not covered by HSS, i.e., in B and V light, is deficient with respect to any reasonable thermal model for the pulsation origin. This demonstrates that the conclusions drawn by HSS, in which a thermal spectrum was assumed, may not be correct.

II. OBSERVATIONS

The observations were made on 1981 February 2–5 UT with the KPNO 1.3 m telescope using an offset guider and the three-channel photometer with two dichroic beam splitters. The two 45° incidence dichroic elements mounted inside the photometer reflect the U light into one side channel (an ITT FW 130 with an S20 photocathode), the $B+V$ light (cyan or C) into a second side channel (with another ITT FW 130 S20), and transmit light with wavelength greater than 5600 Å into a bottom channel (an RCA C31034 with a GaAs photocathode). All three tubes were cooled with dry ice to reduce the dark count. The U-reflecting 45° dichroic

[1]Los Alamos National Laboratory, Los Alamos, New Mexico.
[2]Visiting Astronomer, Kitt Peak National Observatory, which is operated by AURA under contract with the National Science Foundation.

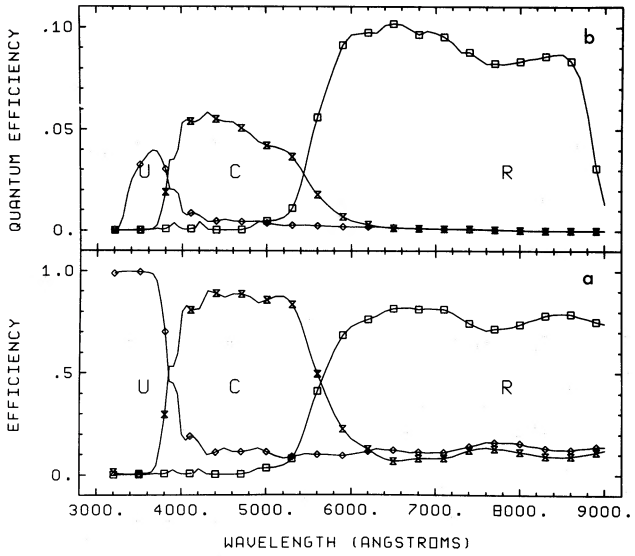

FIG. 1.—(*a*) The splitting of light into three channels (ultraviolet, cyan, and red) by two 45° incidence dichroic elements vs. wavelength. The *U* reflecting dichroic is first in the light path and is followed by the *C* reflecting dichroic. (*b*) The measured quantum efficiencies for the three channel photometer on the KPNO 1.3 m telescope with ITT FW 130 phototubes (S20) for the *U* and *C* side channels and an RCA C31034 (GaAs) tube (#51) for the bottom channel. Both the primary and secondary mirrors on this telescope have a sapphire coating on a silver reflecting surface.

element was similar to that used by HSS except that the dielectric coating was deposited on light-transmitting glass and an antireflection coating was deposited on the back surface (the light exit side) of this glass.

The cyan reflecting dichroic element was fabricated in a similar fashion to the *U*-reflecting dichroic element, but designed for 50% of full transmission near 5500 Å. The efficiency of the two 45° incidence dichroic elements in splitting the light was measured using a CARY 17 transmissivity measuring machine from 3000 Å to 9000 Å. Since the dielectric coatings do not absorb light, the reflectivity can be calculated from the transmissivity measurements. The net splitting of the light by the two elements is plotted in Figure 1*a*.

Short observations of the unpulsed count rates of standard stars and SY Cnc were made with a frequency counter. The amplified photomultiplier pulses were inspected with an oscilloscope at the inputs of the frequency counter and recording system; the cabling was adjusted until pulse reflections (which could cause multiple counting) were eliminated. A journal of the observations is given in Table 1. The count rates measured from the standard stars were used to determine the sensitivity in all three channels. Three standards were observed: HZ 44, G191B2B=EG 247, and L870-2 =EG 11, the spectra of which are well known. The spectrum of HZ 44 closely approximates a 50,000 K blackbody (Oke 1974; Oke and Shipman 1971). The expected flux at the detectors was calculated from the known spectral distributions, the airmasses of the observations (using the extinction coefficients for KPNO; Hayes 1981), the response of the dichroic beam splitter (Fig. 1*a*), the reflectivity of silver for both the primary and secondary mirrors (Allen 1973), and the typical manufacturers' responses of an S20 photocathode for the ITT FW 130's and the GaAs RCA C31034 photocathode. The ratios of expected counts to observed counts for each color channel were consistent between the standards and were averaged to generate a scale factor for each photomultiplier quantum efficiency. The net efficiency curves thus deduced for the three channels (with no atmospheric extinction) are plotted in Figure 1*b*, and the scaling factors are listed in Table 1.

Sky measurements were taken for SY Cnc before and after each long time series run. A 22″ or 28″ aperture was used with the measurements of SY Cnc since the star was very bright. The time series data for the three channels were recorded simultaneously on magnetic tape; the recording on the first night was restricted to only one channel due to technical difficulties (the red channel was chosen because of its high sensitivity). A 10 Hz sampling frequency was used for the time series runs on SY Cnc which varied in length between 2 and 4 hours. The Crab Pulsar was observed on 1981 February 4 UT to check the integrity of the recording/timing system.

The time series for SY Cnc were later summed to 2^{13} or fewer words and then detrended by the subtraction of low-order polynomials. Thin clouds were present in the latter part of the first night's run and at the beginning and end of the second night's run; only the cloud-free portions of these nights were used in the Fourier transforms.

III. ANALYSIS

a) *The Unpulsed Parameters*

A best fit three-parameter spectrum of SY Cnc was used to correct the three-color data for atmospheric extinction. One parameter determined the scaling factor applied to the spectrum of the star near its standstill magnitude (12.3) taken by Wade (1980), and the other two parameters determined linear and quadratic corrections (in frequency, ν) to the resulting spectral intensity, F_ν. The standard star and SY Cnc data for the three bands were converted into $C-U$ and $C-R$ colors and are shown plotted in Figure 2. The origin of the color-color plane was determined using the colors of a flat spectrum (F_ν = constant).

The colors of HZ 44 are in good agreement with a 53,000 K blackbody spectrum (Fig. 2). EG 247 appears to be deficient in cyan light with respect to a blackbody,

TABLE 1

OBSERVING LOG OF STANDARDS AND SY CANCRI

STANDARDS	DATE (1981)	TIME	SCALING FACTORS U	C	R
EG 11	Feb 2	02^h30^m	0.2688	0.4426	1.089
EG 247	Feb 2	03 10	0.3098	0.4204	1.196
HZ 44	Feb 4	12 09	0.2797	0.4144	1.038
HZ 44	Feb 5	12 30	0.2866	0.4146	1.051

Average Results ($U = C = R = 13.90$)
Count Rates (at 0.0 airmass): 1365(U), 3474(C), 8044(R)
Correction from Count Rates to Colors: $(C - R) = -0.91$, $(C - U) = 1.01$

STAR	DATE (1981)	TIME	COUNTS U	C	R	MAGNITUDES U	C	R	TEMPERATURE (Blackbody)
SY Cnc:									
A	Feb 2	07^h30^m	...	...	68,100	...	...	11.47	...
B	Feb 3	06 20	8600	29300	63,600	11.43	11.31	11.54	10874
C	Feb 4	05 29	7500	25900	57,900	11.55	11.43	11.63	10930
D	Feb 4	08 14	7570	26120	56,500	11.58	11.44	11.67	11075
E	Feb 4	10 16	6900	24600	54,950	11.56	11.43	11.66	10841
F	Feb 5	06 50	7450	24100	53,600	11.60	11.53	11.72	11143
G	Feb 5	09 25	6380	22000	50,500	11.74	11.62	11.78	10543
X Leo:									
A	Feb 5	09 48	2140	7860	17300	12.93	12.74	12.94	~11000

TIME SERIES RUNS

Star	Date (1981)	Time	Length	Comments
SY Cnc 001	Feb 2	$6^h07^m15^s$	$3^h.8$	R only, Clouds at end, use first 6393.2 s.
SY Cnc 002	Feb 3	4 42 24	2.6	U, C, R; Clouds at beginning and end, skip first 1638.4 s, analyze 6553.6 s.
SY Cnc 003	Feb 4	5 29 13	0.14	U, C, R; stop to go to CN Ori.
SY Cnc 004	Feb 4	8 13 43	2.0	U, C, R; Clear.
SY Cnc 005	Feb 5	6 49 56	2.1	U, C, R; Clear.
X Leo 002	Feb 5	9 48 19	2.6	U, C, R; Clouds at end, use first 4915.2 s.

while SY Cnc and EG 11 have slight excesses of cyan light. The unpulsed colors of SY Cnc lie close to an 11,000 K blackbody; the best fit blackbody temperatures are shown in Figure 3*a* to be within a few hundreds of degrees of 10,900 K. This temperature is in good agreement with those measured by HSS for the unpulsed light from AH Her on their first four nights of observations.

The mean $C - R$ color is seen in Figure 3*b* to rise from -0.225 to -0.18 in two nights, while the $C - U$ color rises from -0.125 to -0.095, and the C magnitude falls from 11.31 to 11.57. The C magnitude on the first night was estimated from the R observation and the $C - R$ color for the following night. This trend is consistent with the AAVSO visual magnitudes for SY Cnc, which average 11.4 for the first two nights of observations and fall to 11.5 for the last two nights.

b) The Fourier Parameters of the Pulsations in the Three Bands

We detected optical pulsations from SY Cnc in all spectral bands on all nights it was observed. If the optical pulsations are not produced at a single physical location in the binary system, one might expect to see timing differences among the three wavelength bands, caused by (*a*) distinct colors of pulsed emission when combined with (*b*) the light travel time and beaming geometry between the different locations. Such pulse-phase shifts caused by both effects of (*b*) are described for the X-ray/optical pulsar 4U 1626−67 by Middleditch *et al.* (1981). The data were carefully examined for these timing differences, and none were found to within a fraction of a second in each case (5°–10° in phase).

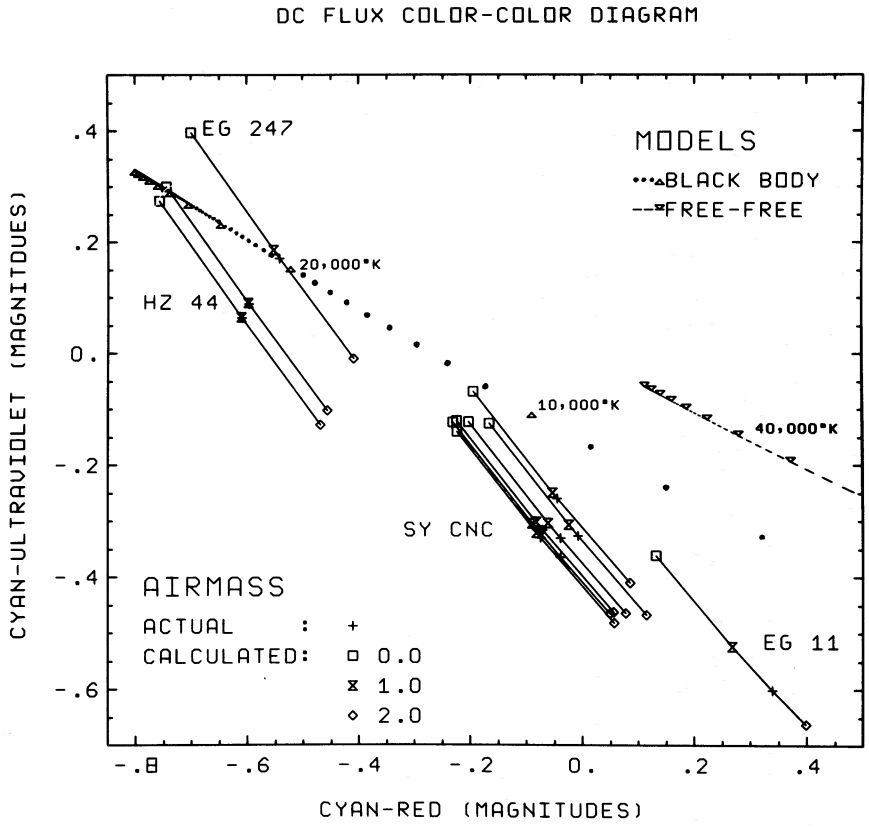

FIG. 2.—The flux results for the standard stars and SY Cnc are plotted on the $(C-R, C-U)$ plane. The actual observations are given by plus signs, and the diamond, hourglass, and square symbols represent the colors reduced to 2.0, 1.0, and 0.0 airmasses, respectively. The loci of blackbody and free-free spectra up to 100,000 K are plotted as dots (every 1000 K) and dashes (every 2000 K) with special symbols every 10,000 K. The blackbody points below 7000 K and free-free points below 22,000 K lie outside the graph. The figure shows the two observations of HZ 44 are in good agreement with a 53,000 K blackbody and SY Cnc to be almost an 11,000 K blackbody. Measurements for the other two standards are also shown.

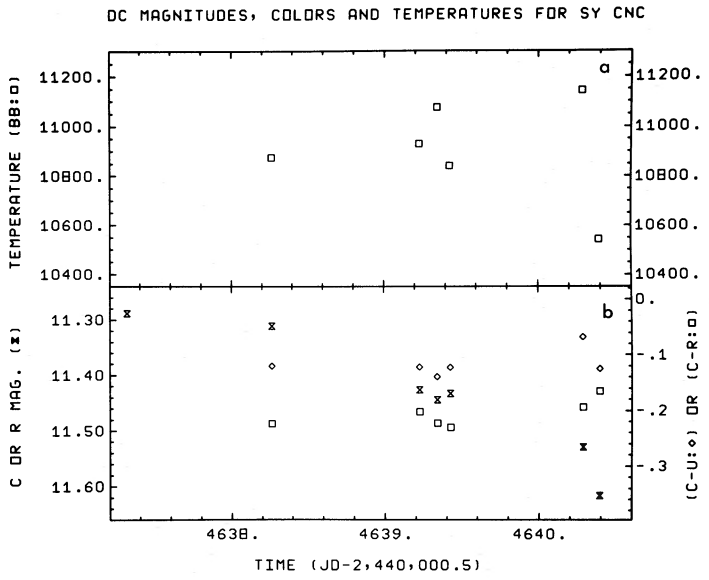

FIG. 3.—(*a*) The best fit blackbody temperature for SY Cnc vs. time. No significant temperature change is observed. (*b*) The unpulsed magnitudes and colors for SY Cnc vs. time. The C magnitude for the first night has been taken from the R magnitude and the $C-R$ color measured for the second night. The star is seen to diminish in intensity while the color changes are much less pronounced.

The Appendix describes the analysis which was applied to the Fourier amplitudes derived from the time series of the three bands. This analysis uses the complex Fourier amplitudes and the first two derivatives with respect to frequency, and transforms these six parameters into six others which represent various physical properties of the pulsations. These parameters are power, phase, $d(\text{power})/df$ ($=0$ at the frequency corresponding to the peak of the power), $d(\text{phase})/df$ (the center of gravity of the pulsations in time), $d^2(\text{power})/df^2$ (the second moment of the pulsations in time) and $d^2(\text{phase})/df^2$ (the change of the pulsation frequency vs time).

Table 2 lists the five free parameters and their errors, as well as the frequency which corresponds to the peak power, the pulsed fractions, and amplitudes. In addition, for each night, mean frequencies and derivatives have been calculated and the phases for each band of pulsation have been evaluated at these average frequencies to allow easier comparison.

The parameters of the three bands listed in Table 2 for a given run are observed to agree within the bounds of statistical fluctuations, except for the pulsed fractions. In fact, many parameters seem to agree better than statistics would predict. The lack of fluctuation stems from the systematics of the time series—the 2% flickering and the occasional unedited thin cloud—being similar in all three colors. Because of this, comparison between parameters for different bands in the same run can usually be made more closely than the local noise power would indicate (see, e.g., Chanan 1978 for a discussion of this effect in DQ Her). Ultimately, the greater change in extinction in the U band tends to limit this advantage.

With the one exception of the pulsation amplitude favoring the second half of run 4, the centroids and rms moments in *time* of the optical pulsations can be seen in Table 2 to characterize a normal (unvarying) coherent oscillation, whereas the frequencies all show systematic changes with time. While the sign of the frequency derivative changes from night to night, the values corresponding to the three bands taken during each night's observation all agree in sign. The low rms moments for the last night's oscillations are due to the longer length of FFT compared to the time series.

Occasionally, small sidelobes appear near the main peaks in the Fourier spectra. Consequently, the Fourier amplitudes derived from each time series were used to test for systematic phase or amplitude modulation as described in Middleditch *et al.* (1981). No systematic modulation was observed; the occasional sidelobes resolve themselves randomly into phase or amplitude modulation power. This is unlike the 9 s X-ray oscillation in the dwarf nova SS Cyg whose sidelobes are predominantly phase modulation in character (Córdova *et al.* 1981).

c) *The Colors of the Pulsations and Flickering*

i) *The Pulsations*

The colors of the pulsations were fixed by the ratios of the pulsed amplitudes determined by the Fourier analysis. The frequencies and their derivatives, pulsed fractions, magnitudes, and colors are plotted in Figure 4. The frequency (Fig. 4*a*) shows an overall monotonic decrease with time of ~ 0.7 mHz day^{-1} ($\sim 10^{-6}$ s s^{-1}), dropping from 35.7 mHz (28 s) on the first night to 33.5 mHz (31 s) on the last night. The frequency of the oscillations is consistent with those reported for this star by Robinson (1973) and Patterson (1981). The monotonic decrease of the pulsation frequency with the star's optical luminosity is consistent with the typical behavior of these oscillations in AH Her and other dwarf novae (see, e.g., Hildebrand *et al.* 1980). The colors have been corrected to 0.0 airmass by self-consistently applying the best quadratic fit (in ν) to the pulsed colors. These fits dip slightly between 5500 and 7500 Å, rising gently toward 9000 Å and steeply toward 3200 Å. The results are consistent with no change in pulsed color during the three nights (Fig. 4*c*).

With only four nights of observations as a sample, we note a possible correlation between the strength of the pulsation and the observed frequency derivative (see Figs. 4*a* and 4*b*), and a probable correlation between the frequency derivative measured on one night and the drop in the frequency by the following night (i.e., the measured derivative for one night minus a constant seems to persist as a real slowdown for a major fraction of the next 24 hours). The pulsation strengths have not been corrected for the power loss due to their df/dt's. For the last night's run this correction would amount to about 15%.

Due to the uncertainty in our knowledge of the spectrum of the optical pulsations in SY Cnc, we feel the colors should not be corrected for atmospheric extinction (as done above). Instead, the models for the pulsations were reddened through the range of airmasses encountered during the runs so that the derived colors could be compared directly to the experimental results.

The models which were used include blackbody and free-free spectra, modulated by (*a*) variation of the radiating area holding the temperature constant (i.e., intensity modulated), and (*b*) variation of the temperature holding the radiating area constant, i.e., (for case *b*)

$$T = T_0 + T_1 \cdot \cos(\omega_p t) \tag{1}$$

$$\begin{aligned} d\,\text{Flux}/dt &= d\,\text{BB}/dT \cdot dT/dt \\ &\approx \text{BB}(\nu, T) \cdot \beta/T \cdot e^{\beta}/(e^{\beta}-1) \cdot \omega_p T_1 \sin(\omega_p t) \\ &= d\,\text{FF}/dT \cdot dT/dt \\ &\approx \text{FF}(\nu, T) \cdot (\beta - 0.5)/T \cdot \omega_p T_1 \sin(\omega_p t), \end{aligned} \tag{2}$$

TABLE 2

PARAMETERS OF THE TIME SERIES RUNS

Run	SY Cnc 1	SY Cnc 2			SY Cnc 4			SY Cnc 5		
Time of Run (s)	6963.2	6553.6			7319.7			7640.0		
Interval of FFT	"	"			7372.8			8192.0		
Mean Frequency (mHz)	35.6975(98)	35.2586(34)			33.8787(60)			33.4169(48)		
" dF/dt ($nHz \cdot s^{-1}$)	4.5(11.6)	-12.5(4.0)			14.7(6.6)			-30.4(5.8)		
Band	R	U	C	R	U	C	R	U	C	R
Phase (mean Freq.)°		-113.3	-100.3	-105.6	5.3	15.3	10.5	2.4	3.4	-6.1
Error		4.3	4.6	4.2	7.8	7.9	8.1	6.6	6.3	6.5
Power/(Local Power)	27.9	88.8	102.9	92.3	27.0	26.3	25.3	37.1	40.8	39.4
(Local Power)/(Poisson)	2.54	1.57	1.89	3.09	1.65	2.18	3.76	1.96	2.11	3.22
Star/(Star+sky) (ϵ)	0.81	0.95	0.95	0.87	0.95	0.95	0.84	0.94	0.94	0.83
Star(counts s^{-1})	66281	8491	29180	63480	7369	25416	55478	7118	23525	51736
Pulsed Fraction (%)	0.088	0.337	0.215	0.184	0.186	0.114	0.091	0.238	0.143	0.124
Error (%)	0.014	0.026	0.015	0.014	0.026	0.016	0.013	0.028	0.016	0.014
Pulsed Amplitude	58.3	28.6	62.6	117.0	13.7	28.8	50.3	17.0	33.6	64.2
Frequency (mHz)	35.6975	35.2612	35.2582	35.2565	33.8791	33.8708	33.8866	33.4186	33.4194	33.4127
Error (mHz)	0.0098	0.0061	0.0059	0.0059	0.0108	0.0102	0.0104	0.0089	0.0078	0.0081
Centroid of Pulsation	0.501	0.493	0.452	0.502	0.627	0.554	0.591	0.496	0.462	0.469
Error	0.044	0.022	0.020	0.021	0.039	0.040	0.041	0.033	0.032	0.033
RMS Moment (Purity)	1.079	1.030	0.987	1.050	0.945	1.009	1.014	0.876	0.951	0.933
Error	0.063	0.033	0.032	0.037	0.064	0.061	0.062	0.059	0.052	0.054
$dF/dt(nHz \cdot s^{-1})$	4.5	-10.0	- 17.2	-10.7	21.2	17.3	7.4	-32.9	-27.6	-32.0
Error	11.5	7.0	7.2	6.7	12.7	11.0	10.8	11.8	8.9	10.0
Flickering: s(%)	0.65	1.52	0.85	0.76	1.15	0.66	0.67	1.81	0.97	0.87
Flickering Amplitude	429	129	248	482	85	167	372	129	227	451

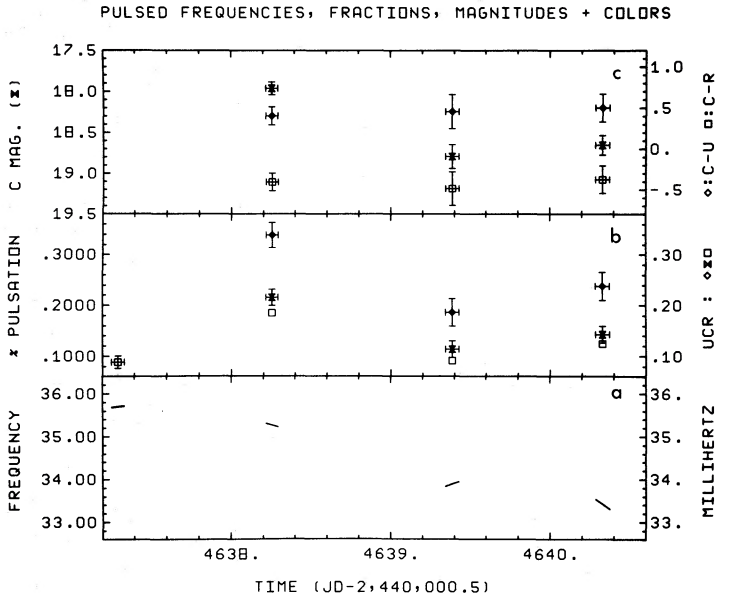

FIG. 4.—(*a*) The observed average frequencies and frequency derivatives, (*b*) the pulsed fractions, and (*c*) the magnitudes and the associated colors for the rapid oscillations of SY Cnc are plotted vs. time.

where T_0 and T_1 are the amplitudes of the steady and oscillating temperature respectively, $\beta = h\nu/kT$, ω_p is the radial frequency of the pulsations, and BB and FF are the usual forms of the blackbody and free-free spectra (cf. Chanan 1978). The modulation of the Gaunt factor in the free-free spectrum has been ignored.

The colors of the pulsation from the three runs and the loci of the four thermal models are plotted on the $(C-R, C-U)$ plane in Figure 5. Comparison between the runs showed that the color differences produced in the models were slight (less than two symbol diameters) and constant over a wide region bracketing the data points. Consequently, only the models constructed for the airmass history of the first (three-channel) night's data are plotted in Figure 5. The data for the following nights are corrected with respect to the models in Figure 5 by using the color differences between these nights and the first night.

The results show a startling deficiency of cyan light in the optical pulsations with respect to both the intensity-modulated and temperature-modulated blackbody models. The clustering of the points shows that the errors assigned to the pulsed colors are conservative, so that even a horizontal translation would not bring the data into good agreement with the (common) Rayleigh-Jeans limit of the two thermal models.

ii) *The Flickering*

The light from SY Cnc was observed to vary aperiodically on a time scale of minutes. To accomodate changes in extinction and sky background over the 2-hour runs, the U, C, and R times series were detrended by subtraction of cubic polynomials; the results for the last night's run (run 5) are plotted in Figure 6. The scale of relative magnitude for this figure is accurate, even though the offset of the scale could only be approximately restored following the polynomial subtraction (compare with the magnitudes in Fig. 2*b* for the last night's run).

A first examination of Figure 6 reveals a remarkable similarity of the flickering in the three wavelength bands. The cross correlation of the three possible pairs of bands show that all of the nonstatistical fluctuations are correlated with a delay time of zero to within a second. A closer look shows the U band varying from magnitude 11.63 to near 11.71, while the C band varies from 11.605 to near 11.65; the U variations thus had almost twice the amplitude of the C variations. The variations of the R band are slightly less than those of the C band. Due to the remarkable similarity of the morphology of the variations for the different bands, they may be quantified by a simple measurement of the fractional variation of the stellar light. More explicitly,

$$s = \left[1/(N-1) \cdot \sum_{k=1}^{N} (y_k - \bar{y})^2 - \bar{y} \right]^{1/2} \Big/ (\bar{y} \cdot \varepsilon) \quad (4)$$

defines the analog of the pulsed fraction, where ε is the estimated mean fraction of the total light which comes from the star, and y_k is the kth data sample after the cubic subtraction and readdition of the average. The values of s are listed in Table 2, as are the absolute rms amplitudes of the flickering.

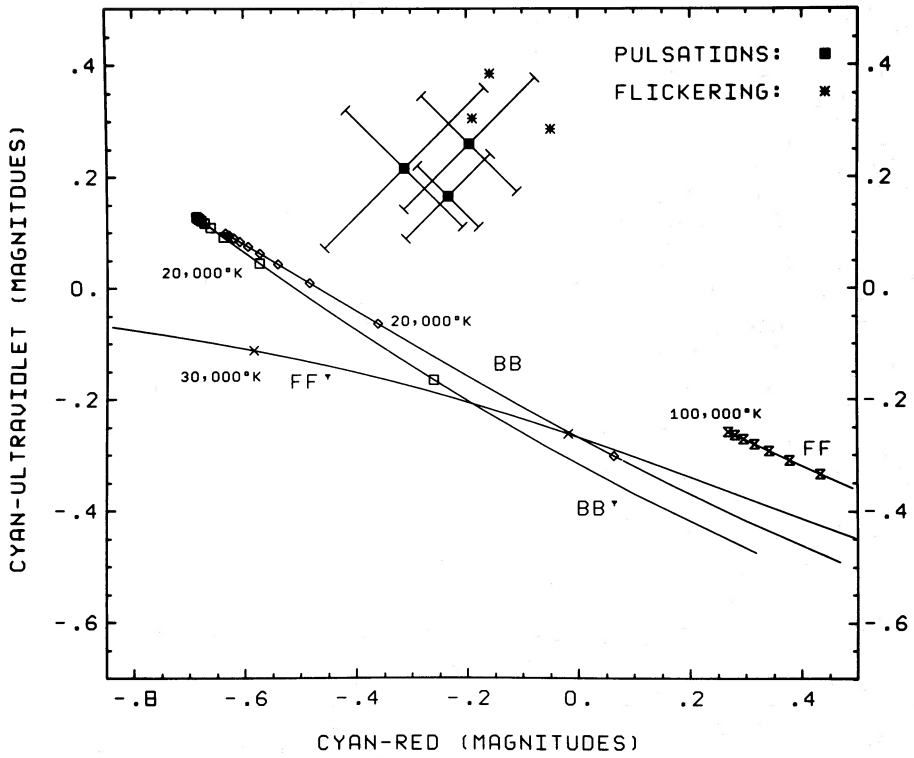

FIG. 5.—The colors of the rapid periodic oscillations and flickering for the three nights of multicolor observations of SY Cnc are plotted on the $(C-R, C-U)$ plane (for clarity, the flickering with no error bars). The loci of the intensity-modulated and temperature-modulated blackbody models are plotted (diamonds and squares shown every 10,000 K), as are the similarly modulated free-free models (hourglasses and ×'s, also every 10,000 K). Due to the uncertainty in the spectra of the pulsations and flickering, the models have been reddened through the airmasses of the observations.

The colors of the flickering, reduced in the same manner as the colors of pulsation, are shown in Figure 5 to cluster even farther from the thermal models than the latter. A correction for gray variations, e.g. clouds, would move the points mostly *upward* in the $(C-R, C-U)$ plane, placing them even farther from the thermal models. No such corrections were applied.

The relative amplitudes for the flickering for runs 2 and 5 are similar; there is a suggestion that the flickering of run 4 is unusual due to its low rms amplitude and redder color. Moreover, the peaks of the cross correlations between the three bands of run 4 are half the peak values for the cross correlations of runs 2 and 5.

IV. DISCUSSION

We have shown that no single-component blackbody or free-free spectrum, modulated in either intensity or temperature, can fit the observed colors of the pulsation in SY Cnc. Even two-component thermal models cannot produce the *abrupt* change that exists between the C and U bands. In the case of the intensity-modulated free-free spectrum, this is easy to see; the monotonically decreasing (with ν) fluxes can never be superposed to increase from the cyan to the ultraviolet. Fitting the pulsed colors with the temperature-modulated free-free spectra is more complicated, since these are the only models which can actually reverse the pulse phase (cf. eq. [3]). For the responses plotted in Figure 1*b*, this phase reversal occurs in the R band between 41,000 K and 42,000 K, in the C band between 61,000 K and 62,000 K, and in the U band between 71,000 K and 72,000 K. However, all such spectra increase at best only linearly with ν (see eq. [3]) and fall off exponentially for $\nu \geq 0.5kTh^{-1}$, so that it is unlikely that any such mixture of spectra can be superposed to simulate the pulsed colors observed in SY Cnc.

Two-temperature blackbody models (modulated in either intensity or temperature) were also unable to produce the observed colors of the optical pulsations. In addition to the two temperatures, the fits had a third parameter to adjust the relative intensities of the spectra. The best two-component fits [those which came closest to the pulsed colors on the $(C-R, C-U)$ plane] yielded a hot component temperature of 20,000 to 50,000 K and a cold component temperature of 1000–2000 K, with an intensity difference of a dozen or so magnitudes in favor of the cool component. Not only are those

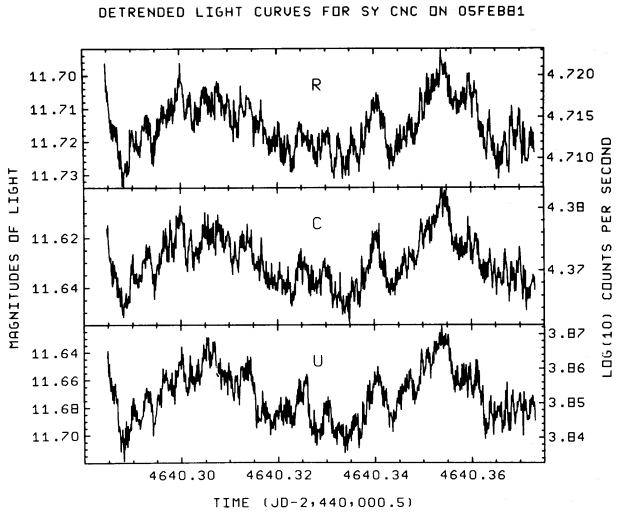

FIG. 6.—The flickering in the U, C, and R time series for SY Cnc on 1981 Feb 5 is shown after the subtraction of cubic polynomials to remove systematic trends of extinction and sky background. Although the offsets of the magnitude scale are therefore slightly inaccurate, the relative scales are still valid. The figure shows the excellent correlation in the time variations of the three colors, with the relative amplitude of the U band variations about twice the amplitudes of the C and R variations.

models unacceptable on the basis of the implied, but unobserved, infrared flux from the source, but the best fits also leave systematic residuals between 0.1 and 0.2 magnitudes in $C-U$ (i.e., not producing enough $C-U$ to fit the data). Because of the low scatter in the measurements of the standard stars, the residuals are much greater than any possible systematic error.

Attempts to fit the pulsed colors with power law models also failed to give reasonable results. The power law index in ν for U to C varies from $n_1=2.5$ for runs 2 and 4 to $n_1=3.0$ for run 5, while an independent fit between C and R gives indices between 0.41 and 0.77. When the index between U and C is fixed at 2.5 or 3.0 and applied across the entire spectrum, the second power law index needed to fit the data varies from $n_2=-1.7$ to $n_2=-14.0$, the highest negative values occurring for the last night's run (5). With an index of 3, the second index for run 5 is -3.9. The Rayleigh-Jeans $n=2$ produces second index values near -14 in all three nights' data–essentially the same catastrophe which occurs when the two-temperature thermal model is applied, or when a thermal model is mixed with a power law. The more extreme flickering colors would, of course, be more difficult to fit with finite spectral indices.

One model which could be made to fit the colors of the pulsations and flickering from SY Cnc is a thermal spectrum in combination with a small amount of free-bound (recombination) radiation from H I and He I. H I has band edges at 8204 Å (Paschen) and 3646 Å (Balmer), while He I has a composite band edge near 8200 Å and a double edge at 3680 Å and 3622 Å (see, e.g., Osterbrock 1974). He II has band edges similar to H I with an extra edge at 5694 Å. If these spectra are modulated in temperature, the largest pulsed amplitudes may occur near the band edges. Since these edges are all outside the cyan bandpass, this interpretation provides a natural mechanism to produce the observed colors of pulsation.

The colors of the 10,000 K H I recombination spectrum from Osterbrock (1974), reddened through the atmosphere, are $C-R=C-U=1.1$, supporting the interpretation of the spectrum as a hot thermal component with a small amount of recombination radiation. In the context of this model, the slight difference in colors between the pulsations and flickering can be attributed to the generation of the pulsation from a region which is more dominated by thermal emission. More work needs to be done on this model to investigate the conditions under which the net pulsation amplitude is enhanced near the band edges and does not, for example, cancel to zero due to opposite flux-level changes on either side of the band edges (as might occur in a temperature-modulated model).

Trailed spectroscopic observations ($\lambda=3550$–4300 Å) of the dwarf nova SS Cyg during its quiescent state by Walker and Chincarini (1968) show evidence for occasional flares which have their maximum amplitude in the far ultraviolet and decrease in intensity (more rapidly than any thermal model would allow) with increasing wavelength. The spectral enhancement due to these flares may persist in the continuum to wavelengths as long as 4100 Å. Walker (1981) has recently demonstrated that the flares in SS Cyg (as well as in AE Aqr and RW Tri) are due chiefly to enhancement in very broad Balmer emission features, with only a small increase in the nearby continuum radiation. These observations are in possible disagreement with the free-bound+thermal emission model suggested here for the SY Cnc pulsations.

The pulsed colors of AH Her measured by HSS may be very close to those of SY Cnc. If we compare the ratio of the pulsed amplitudes, $r_{SY}\equiv a(U)/a(R)$, for SY Cnc to the similar ratio of unpulsed amplitudes, r_{HZ}, for HZ 44, we find $r_{SY}/r_{HZ}=0.80$. The similar ratio, r_{AH}/r_{HZ}, measured by HSS for AH Her was 0.95. Since these ratios have been defined to eliminate the instrumental responses, they should be the same. The small difference might arise from the *UG* 5 blocking filter used by HSS, or from the difference in the widths of the two R bands. Thus, the association of the optical pulsations of AH Her with the white dwarf, made by HSS assuming a simple thermal model, may be in error, if (as in SY Cnc) the pulsed light of AH Her is deficient with respect to thermal models in the $B+V$ band not observed by HSS.

The colors of the 71 s oscillations in the classical nova DQ Her (cf. Chanan, Nelson, and Margon 1978) and the 28 s oscillations in the long-period dwarf nova WZ Sge (cf. Middleditch, Nelson, and Chanan 1978) are only marginally blue. These two oscillations are consistent with temperature-modulated blackbody temperatures of $7{,}7000 \pm 600$ and $8{,}900 \pm 1600$ K, respectively. However, both of these measurements were insensitive at short wavelengths ($\lambda < 4000$ Å) due to the response of the red image tube used. Thus the very blue pulsed component of SY Cnc may not have been observed if it were present in DQ Her and WZ Sge. We also note the relative absence of modulation of the Balmer lines of DQ Her and WZ Sge. The Balmer emission lines of DQ Her, when summed together, show marginally significant 71 s pulsations in *antiphase*, while the less significant results from WZ Sge show that any 10 Å section of $H\beta$ + continuum is less pulsed than 1.4% (the continuum is pulsed at 0.5%). It is possible that the lower recombination rate to the higher levels in hydrogen and helium, and the relatively small amount of free-bound radiation necessary to skew the colors of pulsation away from the loci of the thermal models, conspire to keep the Balmer lines relatively inactive.

As a caution against a uniform interpretation for the origin of all short term variability in dwarf novae, we also report our observation of 160 s quasi-periodic oscillations in X Leo on 1981 February 5 UT, during an optical outburst. Such long-period, quasi-coherent oscillations have been observed previously in several other dwarf novae (Robinson and Nather 1979; also Patterson 1981). The unpulsed colors observed through 1.18 airmass for this system are $(-0.055, -0.40)$, which are fairly close to the colors of SY Cnc (see Fig. 2). However, the pulsed fractions in R, C, and U are $0.38 \pm 0.09\%$, $0.085 \pm 0.04\%$ and $< 0.12\%$ respectively, making the colors of the quasi-periodic oscillation 1.57 for $C - R$ and < 0.04 for $C - U$. The data on X Leo only span ~ 2 hours, so that more three-color observations of quasi-periodicities in dwarf novae are needed to confirm whether the observed red color is a property of the quasi-periodic pulsations in general.

Thus far, attempts to understand the origin of the oscillations have been made by studying their time scales and coherence properties (cf. Robinson and Nather 1979). Recent work at both optical and X-ray wavelengths, however, shows that categorizing pulsations on the basis of these criteria alone leads to ambiguous conclusions (cf. Córdova and Mason 1982). The results presented here suggest that the colors of the oscillations of dwarf novae (and perhaps all cataclysmic variables) might also be useful in distinguishing between possible physical origins of the pulsations.

We would like to thank Dr. J. Barnes and the staff of Kitt Peak National Observatory for their assistance with the instrumentation. A large debt is owed to J. Mattei, E. Mayer, J. Morgan, and the other observers of the AAVSO who kept us informed of the outburst state of several dwarf novae. We are grateful to Dr. R. Carlos for his assistance with the transmissivity measurements of the dichroic elements and to Dr. R. Stiening for sending us the U/C splitting dichroic element. We also thank Dr. W. Priedhorsky and the anonymous referee for their constructive criticisms. An earlier version of this paper was substantially revised at the 1981 Santa Cruz Summer Workshop on Cataclysmic Variable Stars. This work was performed under the auspices of the United States Department of Energy.

APPENDIX

The complex Fourier amplitudes near the frequency of the detected pulsations were analyzed using the continuous Fourier interpolation

$$A_r = \sum_{r-m}^{r+m} A_l e^{ix} \sin x / x; \qquad x \equiv \pi(r - l) \tag{A1}$$

and the first and second derivatives of A_r with respect to the continuous variable, r (r = frequency*$T_{\rm FFT}$, see, e.g., Middleditch *et al.* 1981). The six parameters (the complex element and its two derivatives) can be simply regrouped into six parameters which represent various physical properties of the pulsations (J. Middleditch 1978, unpublished):

1. Power $= A_r A^*_r = \mathrm{Re}\,(A_r)^2 + \mathrm{Im}\,(A_r)^2 \equiv P$.
2. Phase $= \tan^{-1}[\mathrm{Im}\,(A_r)/\mathrm{Re}\,(A_r)] = \phi \pm (2P)^{-1/2}$.
3. $dP/dr = d(A_r)/dr \cdot A^*_r + \mathrm{c.c.} = 0.0$ at the frequency corresponding to the peak of the power (i.e., the best estimate of the frequency of the oscillations.
4. $d\phi/dr = [\mathrm{Re}\,(A_r) \cdot d\,\mathrm{Im}\,(A_r)/dr - d\,\mathrm{Re}\,(A_r)/dr \cdot \mathrm{Im}\,(A_r)]/P$ which has a value of $-\pi$ for steady pulsations ($-180°$ per frequency bin for pulsations whose time centroid is the midpoint of the Fourier time interval). The centroid of the pulsations can be defined as $-d\phi/dr/(2\pi) \pm (24P)^{-1/2}$, where P is the power of the pulsation peak in units of the local average noise power level.

5. $d^2P/dr^2 = d^2A_r/dr^2 \cdot A_r^* + dA_r/dr \cdot dA_r^*/dr + \text{c.c.} = -2\pi^2 P/3$ for steady pulsations (whose mean squared moment in time is $T_{\rm FFT}^2/12$ about the time centroid). The purity or coherence of a pulsations can be defined as

$$\alpha = \left[\left(3/(2\pi^2 P)\cdot -\left(d^2P/dr^2\right)\right]^{1/2} \pm \left[\alpha\cdot(10P)^{1/2}\right]^{-1};\ \langle\alpha\rangle = 1.0.$$

The maximum purity of any pulsed signal is $(3)^{1/2}$; this is also the purity of any of the noncentral lobes of the $\sin^2\pi(f-f_0)/[\pi(f-f_0)]^2$ response function of the Fourier transform for a coherent signal. Thus, the purity measurement may be used to distinguish sidelobes of the response function from sidelobes which may indicate amplitude or phase modulation.

6. $d^2\phi/dr^2 = \text{Re}\,(A_r)\cdot d^2\,\text{Im}\,(A_r)/dr^2 - \text{Im}\,(A_r)\cdot d^2\,\text{Re}\,(A_r)/dr^2$ at the position of the peak power. This parameter can be used to estimate the derivative of the frequency with time:

$$d^2f/dt^2\cdot T_{\rm FFT}^2 \approx Z_{\rm est} = -45/(\alpha\pi)^3\cdot\left(d^2\phi/dr^2\right) \pm \left[90/(P\alpha^4\pi^2) + 81Z_{\rm est}^2/(90P\alpha^4)\right]^{1/2}.$$

This formula for $Z_{\rm est}$ is actually a limit for small arguments. It can be shown that the response of the Fourier power reaches a local minimum of 8.2% response at $Z = 7.3$. The error term proportional to $Z_{\rm est}$ which is added in quadrature to the independent term approximates the diminishing response of the Fourier amplitude's derivatives for moderately large values of df/dt. For very large df/dt's, the power of a coherent signal is spread out over many Fourier amplitudes, and these must be folded with Fresnel integrals in order to bring up the full response.

REFERENCES

Allen, C. W. 1973, *Astrophysical Quantities* (3d ed.; London: Athlone), p. 108.
Chanan, G. A. 1978, Lawrence Berkeley Laboratory Technical Report Number 7227 (thesis).
Chanan, G. A., Nelson, J. E., and Margon, B. 1978, *Ap. J.*, **226**, 963.
Córdova, F. A., Chester, T. J., Mason, K. O., Kahn, S. M., Garmire, G. P., and Middleditch, J. 1981, *Ap. J.*, to be submitted.
Córdova, F. A., Chester, T. J., Tuohy, I. R., and Garmire, G. P. 1980, *Ap. J.*, **235**, 163.
Córdova, F. A., and Mason, K. O. 1982, in *Accretion Driven Stellar X-ray Sources*, ed. W. H. G. Lewin and E. P. J. v.d. Heuvel (Cambridge: Cambridge University Press), in press.
Hayes, D. 1981, private communication.
Hildebrand, R. H., Spillar, E. J., Middleditch, J., Patterson, J. J., and Stiening, R. F. 1980, *Ap. J. (Letters)*, **238**, L145.
Hildebrand, R. H., Spillar, E. J., and Stiening, R. F. 1981, *Ap. J.*, **248**, 268 (HSS).
Middleditch, J., Mason, K. O., Nelson, J. E., and White, N. E. 1981, *Ap. J.*, **244**, 1001.
Middleditch, J., Nelson, J. E., and Chanan, G. A. 1978, *Bull. AAS.*, **9**, 557.
Oke, J. B. 1974, *Ap. J. Suppl.*, **27**, 21.
Oke, J. B., and Shipman, H. L. 1971, in *IAU Symposium 42, White Dwarfs*, ed. W. J. Luyten (Dordrecht: Reidel).
Osterbrock, D. E. 1974, *Astrophysics of Gaseous Nebulae* (San Francisco: W. H. Freeman and Company).
Patterson, J. 1981, *Ap. J. Suppl.*, **45**, 517.
Robinson, E. L. 1973, *Ap. J.*, **183**, 193.
_____. 1976, *Ann. Rev. Astr. Ap.*, **14**, 119.
Robinson, E. L., and Nather, R. E. 1979, *Ap. J. Suppl.*, **39**, 461.
Wade, R. A. 1980, Ph.D. thesis, California Institute of Technology.
Walker, M. F. 1981, *Ap. J.*, **248**, 256.
Walker, M. F., and Chincarini, G. 1968, *Ap. J.*, **154**, 157.
Warner, B. 1976, in *IAU Symposium 73, The Structure and Evolution of Close Binary Systems*, ed. P. Eggleton, S. Mitton, and J. Whelan (Dordrecht: Reidel), p. 85.

F. A. Córdova and J. Middleditch: Los Alamos National Laboratory, M.S. 436, Los Alamos, NM 87545